Towards room-temperature superconductivity in low-dimensional C_{60} nanoarrays: An ab initio study

Dogan Erbahar, Dan Liu, Savas Berber, and David Tománek

Phys. Rev. B **97**, 140505 — Published 9 April 2018

DOI: 10.1103/PhysRevB.97.140505

Towards room-temperature superconductivity in low-dimensional C_{60} nanoarrays: An *ab initio* study

Dogan Erbahar,[1,2,†] Dan Liu,[1,†] Savas Berber,[2] and David Tománek[1,*]

[1] *Physics and Astronomy Department, Michigan State University, East Lansing, Michigan 48824, USA*
[2] *Physics Department, Gebze Technical University, 41400, Kocaeli, Turkey*

(Dated: March 26, 2018)

We propose to raise the critical temperature T_c for superconductivity in doped C_{60} molecular crystals by increasing the electronic density of states at the Fermi level $N(E_F)$ and thus the electron-phonon coupling constant in low-dimensional C_{60} nanoarrays. We consider both electron and hole doping and present numerical results for $N(E_F)$, which increases with decreasing bandwidth of the partly filled h_u and t_{1u} derived frontier bands with decreasing coordination number of C_{60}. Whereas a significant increase of $N(E_F)$ occurs in 2D arrays of doped C_{60} intercalated in-between graphene layers, we propose that the highest T_c values approaching room temperature may occur in bundles of nanotubes filled by 1D arrays of externally doped C_{60} or La@C_{60}, or in diluted 3D crystals, where quasi-1D arrangements of C_{60} form percolation paths.

PACS numbers: 81.05.ub, 73.22.-f, 74.70.Wz, 71.15.Mb

The quest for room-temperature superconductivity has lost nothing of its appeal during the 30-year long intense search following the observation of superconductivity in cuprate perovskites, with the critical temperature T_c rising from the 30-K range in the La-Ba-Cu-O system [1] to 77 K in Y-Ba-Cu-O [2]. Current record T_c values of 133 K in the doped $HgBa_2Ca_2Cu_3O_8$ perovskite [3] and 203 K in sulfur hydride [4] have only been observed under high pressure. Progress in raising T_c significantly further has lagged behind expectations. Whereas the microscopic origin of superconductivity is still being speculated about in high-T_c compounds, the rather high T_c values observed in doped solid C_{60}, possibly even exceeding 60 K [5], result from strong electron-phonon coupling caused by the dynamical Jahn-Teller effect on individual fullerene molecules [6, 7]. In alkali-doped M_3C_{60} molecular solids, T_c could be quantitatively reproduced [6, 7] using the McMillan equation [8]. The key behind a substantial electron-phonon coupling constant is one of its factors, namely a high density of states (DOS) at the Fermi level $N(E_F)$, which depends on the particular element M used to intercalate bulk C_{60}.

Here we propose a way to further increase T_c for superconductivity by increasing $N(E_F)$ and thus the electron-phonon coupling constant λ by reducing the C_{60} coordination number Z in doped low-dimensional C_{60} nanoarrays. We considered intercalation by both electron donors and acceptors, as well as electron doping in a solid formed of La@C_{60} endohedral complexes. We found that $N(E_F)$ increases with decreasing bandwidth of the partly filled h_u HOMO and t_{1u} LUMO derived frontier bands, which may be achieved by reducing the coordination number of C_{60}. Whereas $N(E_F)$ increases significantly by changing from 3D C_{60} crystals to 2D arrays of doped fullerenes intercalated in-between graphene layers, $N(E_F)$ reaches its maximum in doped quasi-1D arrays of C_{60} molecules inside $(10, 10)$ carbon nanotubes (CNTs), forming C_{60}@CNT peapods. Whereas partial filling of the t_{1u}-derived band of C_{60} may be achieved by adsorbing K atoms on the peapod surface, the desired depopulation of the h_u-derived band by adsorbed F is not possible. Our results indicate that the highest T_c value approaching room temperature may occur in electron-doped C_{60} peapod arrays or in diluted 3D crystals, where quasi-1D arrangements of C_{60} form percolation paths.

We performed density functional theory (DFT) calculations to obtain insight into the effect of geometrical arrangement of fullerenes on the electronic structure of C_{60} intercalation compounds. We used the Perdew-Zunger [9] form of the spin-polarized exchange-correlation functional in the local density approximation to DFT, as implemented in the SIESTA code [10], which correctly reproduces the inter-layer spacing and interaction in graphitic structures. The valence electrons were described by norm-conserving Troullier-Martins pseudopotentials [11] with partial core corrections in the Kleinman-Bylander factorized form [12]. We used a double-zeta polarized basis and limited the range of the localized orbitals in such a way that the energy shift caused by their spatial confinement was no more than 10 meV [13]. The Brillouin zone of a 3D lattice of C_{60} molecules was sampled by 10×10×10 k-points, that of a 2D lattice by 10×10 k-points, and that of decoupled 1D chains of C_{60} molecules inside a nanotube by 10 k-points. The DOS was convoluted by 0.02 eV^{-1}. In a periodic arrangement, 1D structures were separated by 15 Å thick vacuum regions and 2D structures by 13 Å thick vacuum regions. The charge density and the potentials were determined on a real-space grid with a mesh cutoff energy of 180 Ry, which was sufficient to achieve a total energy convergence of better than 2 meV/atom.

In alkali-doped M_3C_{60} (M=K, Rb, Cs) fcc crystals, superconductivity with $T_c \lesssim 40$ K has been observed [14] and explained by electron-phonon coupling that is modu-

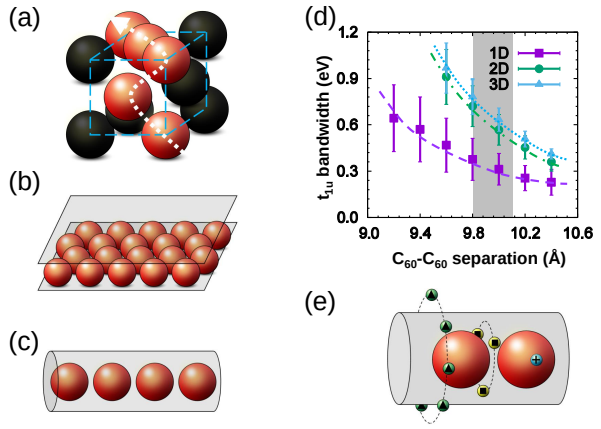

FIG. 1. (Color online) Schematic arrangement of C_{60} molecules in a pristine (a) 3D fcc crystal, (b) 2D triangular lattice, and (c) 1D array inside a (10, 10) carbon nanotube peapod. (d) Width of the t_{1u}-derived band in a 1D, 2D and 3D arrangement of C_{60} molecules as a function of the C_{60}-C_{60} center-to-center separation d_{cc}. Equilibrium values of d_{cc} are affected by the C_{60} orientational disorder, as indicated by the gray strip in (d) for undoped structures. The 'error bars' reflect the effect of changing the C_{60} orientation on the bandwidth. (e) Schematic arrangement of dopant atoms outside the 1D peapod (▲), inside the nanotube but outside the fullerene (■), and inside the fullerene (+). Dark spheres in (a) represent clusters other than C_{60} that separate quasi-1D percolating arrays of fullerenes from the surrounding matrix. The planes in (b) are only a visual aid.

lated by the lattice constant [6, 7]. The same behavior is expected to occur in the isoelectronic La@C_{60} that has been isolated from raw soot [15] and found to be stable [16]. When exohedrally doped M_3C_{60} crystals are exposed to ambient or harsh conditions, atoms from the environment may penetrate deep inside the lattice, react with the M atoms and destroy superconductivity. This is much less likely to occur in endohedrally doped La@C_{60} crystals, since the dopant La atoms are enclosed inside the protective C_{60} cage. As mentioned above, superconductivity in 3D M_3C_{60} crystals is caused by strong electron-phonon coupling related to a dynamical Jahn-Teller effect on individual C_{60} cages, made possible by retardation. The dominant role of the intercalated alkali atoms is to partly fill the t_{1u} LUMO of C_{60} that broadens to a narrow band in the M_3C_{60} molecular solid. Changes in T_c caused by pressure or changing the element M can be traced back to changes in the electron-phonon coupling constant $\lambda = VN(E_F)$ in the McMillan equation [6–8]. Since the on-ball Bardeen-Pines interaction V does not change, λ is proportional to the C_{60}-projected DOS at the Fermi level $N(E_F)$, which – for electron doping – is roughly inversely proportional to the width of the t_{1u}-derived band. In hole-doped C_{60}, E_F is expected to be lowered into the h_u-derived band with an even higher $N(E_F)$ value, which may be the cause of the high value $T_c \gtrsim 60$ K that has been reported earlier [5].

All experimental strategies used so far to raise T_c have been based on increasing the C_{60}-C_{60} separation d_{cc} in a 3D fcc crystal, which would lower the width of the LUMO- and HOMO-derived bands and thus increase $N(E_F)$ in doped crystals. Our approach is quite different [17]: we consider increasing $N(E_F)$ by reducing the number of C_{60} nearest neighbors. As seen in Fig. 1(a), this may be achieved simply in a 3D crystal by mixing C_{60} with clusters of similar size that do not interact with C_{60}, such as BN fullerenes. In this case, the lowered C_{60} coordination number would decrease the width of the t_{1u} and h_u derived bands and thus increase $N(E_F)$ in doped crystals. Other C_{60} arrangements with a lower Z include 2D arrays of C_{60} that could possibly be intercalated in graphite [18, 19], as seen in Fig. 1(b), or 1D arrays of C_{60} in C_{60}@CNT peapods [20–22] shown in in Fig. 1(c). As seen in Fig. 1(d), the width of the t_{1u}-derived band decreases both with increasing the C_{60}-C_{60} separation and with the reduction of dimensionality that translates to the reduction of Z, with 1D arrangements appearing optimal. Since superconductivity is suppressed in truly 1D systems according to the Mermin-Wagner theorem [23], we consider bundles of weakly interacting peapods in-

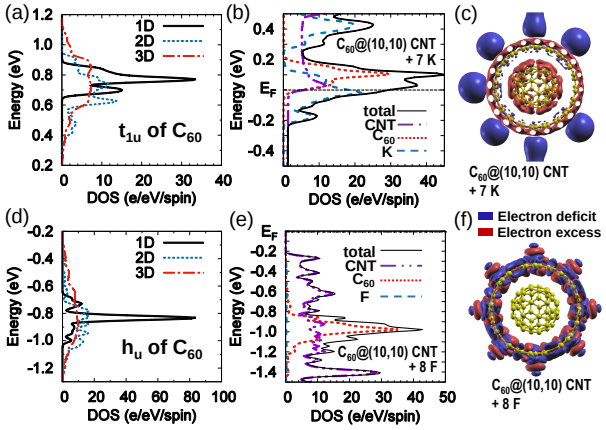

FIG. 2. (Color online) Density of states (DOS) and charge redistribution in doped C_{60} crystals. (a) DOS of the t_{1u} LUMO-derived bands of C_{60} in 1D, 2D and 3D periodic C_{60} arrangements for the C_{60}-C_{60} separation $d_{cc} = 9.8$ Å. (b) Total and projected DOS of a C_{60}@(10, 10) CNT peapod doped externally by 7 K donor atoms per C_{60}. (c) Charge density difference $\Delta\rho = \rho_{tot}(C_{60}@CNT{+}7K) - \rho_{tot}(C_{60}@CNT) - \sum_{at} \rho_{tot}(K\ atom)$. (d) DOS of the h_u HOMO-derived bands of C_{60} in 1D, 2D and 3D periodic C_{60} arrangements for the C_{60}-C_{60} separation $d_{cc} = 9.8$ Å. (e) Total and projected DOS of a C_{60}@(10, 10) CNT peapod doped externally by 8 F acceptor atoms per C_{60}. (f) Counterpart of (c) for C_{60}@CNT+8F. In (c) and (f), blue contours for electron deficit are shown for $\Delta\rho = -3.0\times10^{-3}$ e/bohr^3 and red contours for electron excess are shown for $\Delta\rho = +3.0\times10^{-3}$ e/bohr^3. All energies are with respect to E_F.

stead of isolated 1D peapods. As we will show in the following, the main role of the nanotube in these systems is to provide a suitable enclosure that aligns C_{60} molecules and protects them from the ambient. Due to their weak interaction, bundles of nanotubes have a very similar DOS as isolated nanotubes. Since the same applies to peapods, we will consider an isolated peapod a valid representative of a peapod bundle from the viewpoint of electronic structure.

Even in pristine systems with no intercalants, we found the C_{60}-C_{60} separation d_{cc} to depend on the C_{60} orientation and the dimensionality of the system. Different fullerene orientations, each with a specific optimum d_{cc} value, were found to be energetically degenerate within $\lesssim$2 meV/atom and separated by minute activation barriers. At nonzero temperatures during synthesis and observation, the fullerenes will explore these orientational degrees of freedom causing orientational disorder and changing d_{cc}, as observed in the 3D lattice [24]. The equilibrium value of d_{cc} decreases by $\approx$0.1 Å and its orientational dependence increases when reducing the dimensionality to 2D and 1D. Also in view of the soft C_{60}-C_{60} interaction, we always expect a nonzero range of d_{cc} values in any experimental sample. In pristine C_{60}, we expect d_{cc} values roughly covering the $9.8-10.1$ Å range shown by the dark band in Fig. 1(d).

As seen in Fig. 1(e), the geometry is more complex in alkali intercalated peapods, where intercalant atoms may occupy sites outside the nanotube, inside the nanotube but outside C_{60}, or inside the C_{60} molecule such as the La@C_{60} metallofullerene [16]. Since also these sites are energetically near-degenerate, the precise geometry may be barely controllable during synthesis. In the 3D M_3C_{60} system, moreover, d_{cc} has been found to increase from 9.8 Å to 10.3 Å with increasing atomic number of the alkali element M [6]. We find a similar M-dependent increase in d_{cc} also in 2D and 1D systems, where M atoms separate fullerenes. 1D peapods with the narrowest bandwidth and potentially highest $N(E_F)$ could be doped by donor or acceptor atoms. For most of this study, we will focus on donor doping, causing partial filling of the t_{1u}-derived band, and will show later that acceptor doping may be hard to achieve.

The DOS shape of the t_{1u} LUMO-derived band in quasi-1D, 2D triangular and 3D fcc lattices of C_{60} is depicted in Fig. 2(a) and that of the h_u HOMO-derived band in the same lattices is shown in Fig. 2(d). Clearly, the DOS at E_F reaches its maximum near half-filling of these bands in quasi-1D structures. Since the t_{1u} LUMO-derived band holds up to 6 electrons and the h_u HOMO-derived band up to 10 electrons, half-filling of these bands requires either 3 extra electrons or depletion of 5 electrons from each C_{60}. Comparing our results in Figs. 2(a) and 2(d), we note that acceptor doping – if achievable – would result in a significantly higher $N(E_F)$ than donor doping.

The calculated DOS of a C_{60}@$(10,10)$ peapod doped externally by 7 K atoms per C_{60} is shown in Fig. 2(b) and the DOS of the corresponding peapod doped externally by 8 F atoms per C_{60} is shown in Fig. 2(e). Comparing the partial densities of states in these two cases, we conclude that C_{60}-derived states are barely affected by those of the surrounding nanotube due to a very small hybridization. In the case of donor doping by K depicted in Fig. 2(b), we clearly observe partial filling of the t_{1u}-derived band of C_{60} as well as the nearly-free electron bands of the $(10,10)$ nanotube [25]. To get a better feel for the charge flow in the system, we plotted the charge density difference defined by $\Delta\rho = \rho_{tot}(C_{60}@CNT{+}7K) - \rho_{tot}(C_{60}@CNT) - \sum_{at}\rho_{tot}(K\ atom)$ in Fig. 2(c). Obviously, there is a net electron flow from K atoms to the C_{60}@$(10,10)$ peapod, with the excess charge accommodated both by the C_{60} and the nanotube. Integration of the C_{60}-projected DOS in Fig. 2(b) up to E_F indicates a partial population of the t_{1u}-derived band by 0.4 electrons.

The calculated DOS of an acceptor-doped peapod, shown in Fig. 2(e), presents a very different picture. We selected F as a suitable electron acceptor due to its high electronegativity. Unlike in previous studies of acceptor-doped C_{60}, where covalently bonded halogen atoms disrupted the π-electron network on the molecules [26], F atoms were bonded on the outside of the nanotube surrounding C_{60} molecules. Thus, we found the h_u-derived band of C_{60} to be essentially unaffected by the presence of the surrounding nanotube and the 8 F atoms per C_{60} outside the nanotube, but the C_{60} molecules remained charge neutral. The h_u-derived narrow band band remained completely filled, located about 1 eV below E_F. We found F atoms to bind covalently to the outside of the nanotube, causing pyramidalization, disrupting its π-electron network and opening up a gap at the Fermi level, which turned the system into a semiconductor. This can be clearly seen when inspecting the charge flow in this system in Fig. 2(f). We found F atoms to strongly hybridize with the C atoms of the tube, redistributing the charge only within the F/CNT subsystem, with no effect on the net charge of C_{60}. Since hole doping of C_{60} appears very difficult, we will focus on electron doping of the t_{1u}-derived band of C_{60} chains in the following.

As mentioned earlier, the electronic band structure of C_{60} arrays should depend to a nontrivial degree on the orientation of the C_{60} molecules that will affect their interaction [27]. We studied 5 different orientations, identified in Fig. 3(a), which result in a different degree of inter-ball hybridization. Due to their energetic near-degeneracy, we expect many C_{60} orientations to coexist within a quasi-1D C_{60} array inside a peapod. The DOS for a chain of C_{60} molecules at different orientations and the C_{60}-C_{60} separation $d_{cc} = 9.8$ Å is shown in Fig. 3(b). We note that the maximum DOS value changes significantly with orientation. Therefore, in Fig. 3(c), we plot-

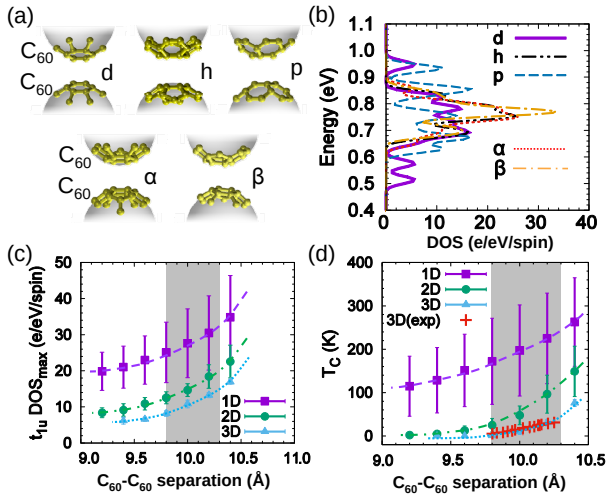

FIG. 3. (Color online) Properties of 1D arrays of C_{60} molecules found in CNT peapods. (a) Ball-and-stick models of different atomic arrangements at the C_{60}-C_{60} interface. Considered are double-bonds facing double-bonds (d), hexagons facing hexagons (h), pentagons facing pentagons (p). α and β arrangements are obtained by a 90° rotation of C_{60} molecules in p arrangement about two different axes that are orthogonal to the chain axis and to each other. (b) DOS of the t_{1u} LUMO-derived bands of C_{60} for the C_{60} orientations, defined in (a), at the C_{60}-C_{60} separation $d_{cc} = 9.8$ Å. All energies are with respect to E_F. (c) Maximum DOS value of t_{1u}-derived bands in 1D, 2D and 3D crystals of C_{60}. The 'error bars' reflect the effect of changing the C_{60} orientation. (d) Critical temperature for superconductivity T_c based on the McMillan equation (1) and using $N(E_F)$ from (c). Equilibrium values of d_{cc} are affected by the C_{60} orientational disorder, as indicated by the gray strips in (c) and (d) for doped structures. The lines in (c) and (d) are guides to the eye.

ted the range of achievable maxima of $N(E_F)$ as 'error bars' for different C_{60}-C_{60} orientations. Depending on the exact position of the intercalant atoms and fullerene orientation, we found the optimum C_{60}-C_{60} separations to cover the range d_{cc}≈9.8 − 10.3 Å, indicated by the gray strip in Fig. 3(c). Higher d_{cc} values than in pristine peapods, achieved in case that the fullerenes are separated by heavy alkalis such as Cs, result in very high values of $N(E_F)$ for favorable C_{60} orientations.

To estimate the critical temperature for superconductivity T_c, we used McMillan's equation [6–8]

$$T_c = \frac{\hbar\omega_{log}}{1.2k_B} \exp\left[\frac{-1.04(1+\lambda)}{\lambda - \mu^* - 0.62\lambda\mu^*}\right] . \qquad (1)$$

This equation describes the solution of the Eliashberg equations in superconductors with a strong electron-phonon coupling ($\lambda \lesssim 2$) in a semi-empirical way that is physically appealing. It also has been found to correctly reproduce the observed T_c values in M_3C_{60} solids as a function of the C_{60}-C_{60} separation [7], shown by the data points for 3D systems in Fig. 3(d). We used the parameters of Ref. [7], namely $\hbar\omega_{log}/k_B = 2800$ K, $\mu^* = 0.2$ for the effective mass and $V = 52$ meV for the Bardeen-Pines interaction, which are not affected by the averaged local arrangement of C_{60} molecules. Using $\lambda = VN(E_F)$ for the electron-phonon coupling constant, we were able to convert $N(E_F)$ values for 3D, 2D and quasi-1D systems with different C_{60}-C_{60} distances and C_{60} orientations to potentially achievable T_c values and present our results in Fig. 3(d). Since dynamical orientational disorder and resulting fluctuations in the C_{60}-C_{60} distance are a natural phenomenon that is particularly prominent in realistic 1D systems, we can estimate ranges of d_{cc} and T_c values at best. Our estimates indicate that, in the best imaginable scenario, T_c near room temperature may be achievable using bundles of donor-doped peapods.

Clearly, there are limits to the range of C_{60}-C_{60} separations d_{cc} compatible with superconductivity. Increasing d_{cc} decreases the inter-ball hopping integral t, while not affecting the on-ball Coulomb integral U. At large C_{60}-C_{60} separations, the U/t ratio should increase beyond a critical value that would change doped C_{60} from a metal to a Mott-Hubbard insulator [28, 29].

In summary, we have proposed a viable way to further increase T_c for superconductivity by increasing the C_{60}-projected density of states (DOS) at the Fermi level $N(E_F)$ and thus the electron-phonon coupling constant in doped low-dimensional C_{60} nanoarrays. We considered intercalation by both electron donors and acceptors, as well as electron doping in a solid formed of La@C_{60} endohedral complexes. We found that $N(E_F)$ increases with decreasing bandwidth of the partly filled h_u HOMO- and t_{1u} LUMO-derived frontier bands, which may be achieved by reducing the coordination number of C_{60}. $N(E_F)$ increases significantly by changing from 3D C_{60} crystals to 2D arrays of doped fullerenes intercalated in-between graphene layers and reaches its maximum in doped quasi-1D arrays of C_{60} molecules inside C_{60}@CNT peapods formed of $(10, 10)$ CNTs. Whereas partial filling of the t_{1u}-derived band may be achieved by adsorbing alkali atoms outside the 1D peapod, the desired depopulation of the h_u-derived band could not be achieved by F atoms adsorbed on the nanotube surrounding the C_{60} molecules. Our results indicate that the highest T_c values may occur in electron-doped C_{60} peapods containing Cs or in dilute 3D crystals, where quasi-1D arrangements of C_{60} form percolation paths. Only experimental evidence will show if low-dimensional arrays of doped C_{60} will become superconducting with T_c approaching room temperature, or rather turn to a Mott-Hubbard insulator.

ACKNOWLEDGMENTS

D.E. acknowledges the hospitality of MSU, where this research was performed. D.L. and D.T. acknowledges financial support by the NSF/AFOSR EFRI 2-DARE grant number EFMA-1433459. Computational resources have been provided by the Michigan State University High Performance Computing Center.

† These two authors contributed equally.

* E-mail: tomanek@msu.edu

[1] J. G. Bednorz and K. A. Müller, Z. Phys. B **64**, 189 (1986).

[2] M. K. Wu, J. R. Ashburn, C. J. Torng, P. H. Hor, R. L. Meng, L. Gao, Z. J. Huang, Y. Q. Wang, and C. W. Chu, Phys. Rev. Lett. **58**, 908 (1987).

[3] C. W. Chu, L. Gao, F. Chen, Z. J. Huang, R. L. Meng, and Y. Y. Xue, Nature **365**, 323 (1993).

[4] A. Drozdov, M. Eremets, I. Troyan, V. Ksenofontov, and S. Shylin, Nature **525**, 73 (2015).

[5] L. Song, K. Fredette, D. Chung, and Y. Kao, Solid State Commun. **87**, 387 (1993).

[6] M. Schluter, M. Lannoo, M. Needels, G. A. Baraff, and D. Tomanek, Phys. Rev. Lett. **68**, 526 (1992).

[7] M. Schluter, M. Lannoo, M. Needels, G. A. Baraff, and D. Tomanek, J. Phys. Chem. Solids **53**, 1473 (1992).

[8] W. L. McMillan, Phys. Rev. **167**, 331 (1968).

[9] J. P. Perdew and A. Zunger, Phys. Rev. B **23**, 5048 (1981).

[10] J. M. Soler, E. Artacho, J. D. Gale, A. García, J. Junquera, P. Ordejón, and D. Sánchez-Portal, J. Phys: Cond. Mat. **14**, 2745 (2002).

[11] N. Troullier and J. L. Martins, Phys. Rev. B **43**, 1993 (1991).

[12] L. Kleinman and D. M. Bylander, Phys. Rev. Lett. **48**, 1425 (1982).

[13] E. Artacho, D. Sánchez-Portal, P. Ordejón, A. García, and J. M. Soler, Phys. Stat. Sol. **215**, 809 (1999).

[14] A. F. Hebard, M. J. Rosseinsky, R. C. Haddon, D. W. Murphy, S. H. Glarum, T. T. M. Palstra, A. P. Ramirez, and A. R. Kortan, Nature **350**, 600 (1991).

[15] H. Shinohara (private communication).

[16] J. Guan and D. Tománek, Nano Lett. **17**, 3402 (2017).

[17] R. F. Service, Science **292**, 45 (2001).

[18] S. Saito and A. Oshiyama, Phys. Rev. B **49**, 17413 (1994).

[19] M. Fuhrer, J. Hou, X.-D. Xiang, and A. Zettl, Solid State Commun. **90**, 357 (1994).

[20] S. Okada, Phys. Rev. B **72**, 153409 (2005).

[21] V. Timoshevskii and M. Côté, Phys. Rev. B **80**, 235418 (2009).

[22] T. Koretsune, S. Saito, and M. L. Cohen, Phys. Rev. B **83**, 193406 (2011).

[23] N. D. Mermin and H. Wagner, Phys. Rev. Lett. **17**, 1133 (1966), and *ibid.* **17**, 1307 (1966)(E).

[24] P. A. Heiney, J. E. Fischer, A. R. McGhie, W. J. Romanow, A. M. Denenstein, J. P. McCauley Jr., A. B. Smith, and D. E. Cox, Phys. Rev. Lett. **66**, 2911 (1991).

[25] S. Okada, S. Saito, and A. Oshiyama, Phys. Rev. Lett. **86**, 3835 (2001).

[26] Y. Miyamoto, A. Oshiyama, and S. Saito, Solid State Commun. **82**, 437 (1992).

[27] M. P. Gelfand and J. P. Lu, Phys. Rev. Lett. **68**, 1050 (1992).

[28] A. Y. Ganin, Y. Takabayashi, P. Jeglič, D. Arčon, A. Potočnik, P. J. Baker, Y. Ohishi, M. T. McDonald, M. D. Tzirakis, A. McLennan, G. R. Darling, M. Takata, M. J. Rosseinsky, and K. Prassides, Nature **466**, 221 (2010).

[29] Y. Nomura, S. Sakai, M. Capone, and R. Arita, Science Adv. **1**, e1500568 (2015).